Journal of Metals, Materials and Minerals, Vol. 32, No. 1, pp. 86-92, 2022

Sintering behavior of nanostructured β-CPP powder obtained from avian eggshell waste

Bruno Silvano SILVA[1], Tarcília Henrique Amaral CORRÊA[1], Rômulo Leite LOIOLA[1], and José Nilson França HOLANDA[1,*]

[1] *Northern Fluminense State University, Advanced Materials Laboratory/GMCer, Campos dos Goytacazes, RJ, Brazil*

***Corresponding author e-mail:** holanda@uenf.br

Received date:
9 June 2021
Revised date
22 January 2022
Accepted date:
30 January 2022

Keywords:
β-CPP;
Eggshell waste;
Sintering;
Properties;
Microstructure

Abstract

In this work the sintering behavior of a nanostructured β-calcium pyrophosphate (β-CPP) powder derived of avian eggshell waste was investigated. The β-CPP pellets were prepared by uniaxial pressing and sintered in air for 2h at temperatures ranging from 600°C to 1200°C. The sintering behavior was evaluated in terms of linear shrinkage, water absorption, apparent porosity, apparent density, tensile strength, FTIR (Fourier-transform infrared) analysis, and microstructural analysis via SEM (scanning electron microscopy). The results showed that the nanostructured β-CPP powder presented different behaviors with increasing sintering temperature. It was found that sintering at higher temperatures led to greater densification of the β-CPP pellets (92.56% of theoretical density when sintered at 1000°C). However, SEM micrographs of the fractured surfaces of the sintered β-CCP pellets showed the presence of micro-cracks that negatively impact the mechanical strength. Hence, it was concluded that the sintering temperature of 900°C was found to be the most suitable in terms of densification, mechanical strength, and sintered microstructure for the production of β-CPP bioceramic pellets derived of avian eggshell waste for potential medical application.

1. Introduction

The calcium phosphate bioceramics (Ca-P) are of great interest in research and medical applications, and can be used in the manufacture of prostheses and grafts [1,2]. Special attention has been given to hydroxyapatite (HAp,$Ca_{10}(PO_4)_6(OH)_2$), which has a mineral composition similar to that of natural teeth and bone [2-4]. However, it is also noted that slow biodegradation is considered an important limitation to its wider use in biomedical applications [5,6]. This fact has aroused great research interest in other pure or multiphasic calcium phosphate bioceramics, which can overcome this deficiency of pure hydroxyapatite.

The calcium pyrophosphate (CPP, $Ca_2P_2O_7$) is considered the lowest linear polyphosphate with a Ca/P ratio equal to 1.0. It has attracted great interest as a grafting material and/or bone substitute with good biocompatibility characteristics [6-11]. The calcium pyrophosphate may be crystallized into three polymorphic forms (γ-CPP, β-CPP, and α-CPP), but the β-CPP is that of most practical interest in biomedical applications. β-CPP powders have been synthesized using a variety of calcium sources and methods [7-11].

The pure β-CPP powders are usually synthesized using a high purity calcium precursor source. However, the traditional commercial calcium precursors (calcium carbonate, calcium nitrate, calcium hydroxide, etc.) used to obtain calcium phosphate based bioceramics are consider very costly [12,13]. On the other hand, the high daily consumer of avian eggs generates huge volumes of avian eggshell waste worldwide. Such a solid waste when improperly disposed of causes serious environmental and public health problems [14]. Importantly, the clean eggshell waste (without the inner organic membrane) corresponds to calcified eggshell (inorganic fraction) made of calcium carbonate in the form of calcite ($CaCO_3$) [15,16]. This indicates that the avian eggshell waste has high potential to be a low cost, renewable high purity calcium source to produce β-CPP powder. In fact, the avian eggshell waste has been recently tested to obtain pure β-CPP nanopowder, displaying promising results [17].

It is well known that the calcium phosphate bioceramics have poor mechanical properties, which limit their use in low or non-load bearing applications [2]. This has stimulated the study of the sintering behavior and improvement of the mechanical properties of calcium phosphate bioceramics. The sintering of calcium phosphate bioceramics is mainly done via the conventional sintering process, but other methods such as two-step sintering, hot isostatic pressing, microwave sintering, and spark plasma sintering have also been tested [18-23]. Such methods have been used mainly for the sintering of HAp, β-TCP, and HAp/β-TCP mixtures. On the other hand, only a few reports on the sintering behavior of β-CPP powders are available. Bian *et al.* [24] investigated the conventional sintering behavior of CPP ($Ca_2P_2O_7$) with different phase composition synthesized via solid-state reaction method using high-purity traditional $CaCO_3$ source. The CPP pellets were sintered between 1150°C and 1290°C for 2 h to 4 h. It was found that the β-CPP phase densifies much faster than α-CPP phase and α-CPP + β-CPP mixture. In addition, β-CPP could be sintered at 1150°C/2 h with high bulk density (98% of theoretical density) and α-CPP could be sintered at 1290°C/4 h with bulk density of 95.8% of theoretical density. Safronova *et al.* [9]

investigated the conventional sintering behavior of β-CPP nanopowders synthesized via wet precipitation method using calcium nitrate tetrahydrate as calcium source. The sintered β-CPP pellets achieved 87% of theoretical density at 900°C and 79% of theoretical density at 1000°C and 1100°C. Wang *et al.* [25] pointed out that when 1% strontium-doped β-CPP pellets (porous scaffolds) were sintered between 700°C and 900°C for 3 h, the density of the sintered pellets increased with the increase of sintering temperature. It was found that the density of the sintered pellets increased from 79.61% theoretical density at 700°C to 84.14% theoretical density at 900°C. However, to the best of our knowledge, the sintering behavior of nanostructured pure β-CPP powder derived from avian eggshell waste has not been investigated yet. In particular, it should be highlighted that the use of avian eggshell waste as a renewable high purity calcium precursor for the production of β-CPP pellets is of high economic and environmental interest [26]. As a fact matter, the use of avian eggshell waste can both reduce the amount of waste to be disposed and reduce the costs of using expensive and high purity calcium precursors to produce β-CPP pellets for medical applications.

The aim of this work was to investigate the sintering behavior of nanostructured β-CPP bioceramic powder derived from avian eggshell waste. Special emphasis is given to the effects of the sintering temperature on the physical and mechanical properties, densification, and microstructural evolution of β-CPP bioceramic.

2. Experimental

The flow diagram of production of the β-CPP pellets is shown in Figure 1. In this work β-CPP powder was prepared by a simple wet precipitation method using avian eggshell waste as an alternative calcium precursor source. Details on the β-CPP powder synthesis process have been described elsewhere [17]. The synthesized powder with average crystallite size of 62.3 nm was essentially composed of tetragonal structured β-CPP (ICSD-PDF 01-071-2123) [17]. The SEM micrograph of the as-prepared β-CCP nanopowder is shown in Figure 2.

The β-CPP powder was uniaxially pressed at 125 MPa to produce disk-shaped pellets (diameter of 10 mm), and then dried at 110°C for 24 h. Finally, the green β-CPP pellets (four test specimens for each temperature) were sintered in air at soaking temperatures varying from 600°C to 1200°C for 2 h in an electrical kiln. The sintering step was carried out under air atmosphere with heating rate of 20°C·min^{-1}.

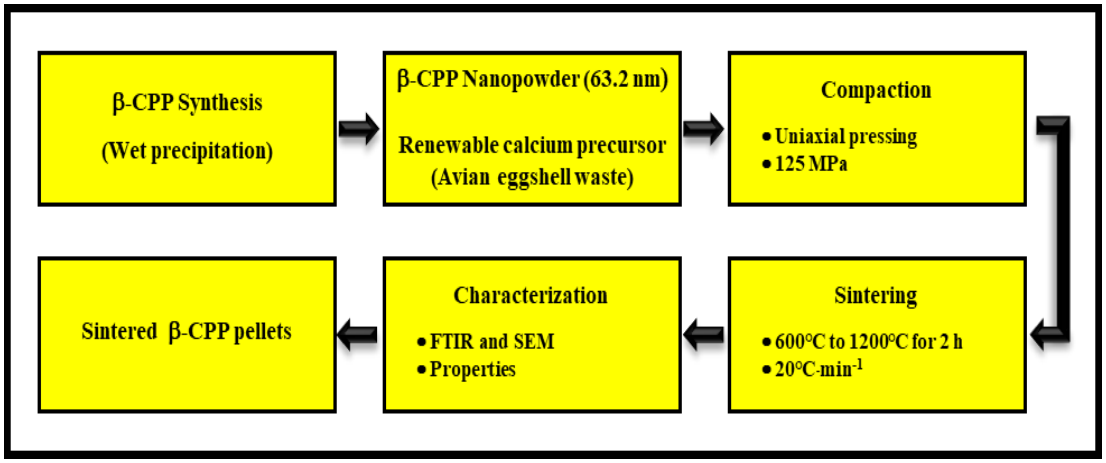

Figure 1. Production flow diagram of β-CPP pellets derived from avian eggshell waste.

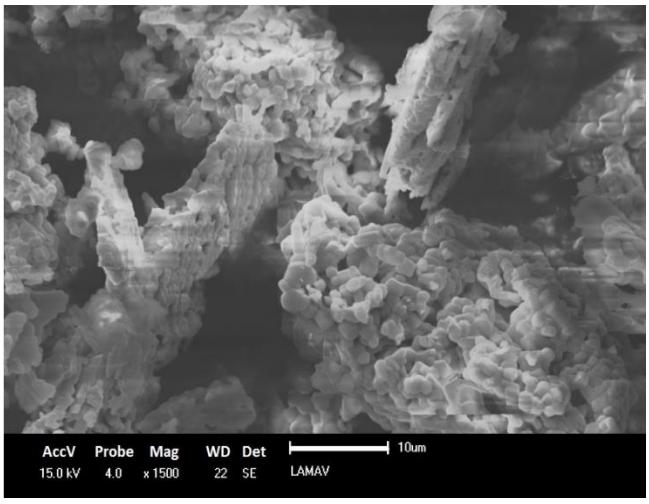

Figure 2. SEM micrograph of β-CPP powder derived from eggshell waste.

The sintering behavior was monitored in terms of linear shrinkage, water absorption, apparent porosity, apparent density, mechanical strength, FTIR analysis, and microstructural evolution via scanning electron microscopy.

The linear shrinkage values of the sintered pellets were obtained by measuring the diameter of the disk specimens before and after sintering step using a caliper with a precision of ±0.01 according to ASTM C 326-09. The Water absorption, apparent porosity, and apparent density values were determined according to ASTM C 373. In this work the mechanical strength of the sintered pellets was determined in terms of tensile strength by the diametral compressive method [27,28] due to the sample geometry (disk with diameter of 10 mm) by using an universal testing machine (model 5582/100 kN, Instron). The crossbar speed was hold at 1.0 mm·min^{-1} for all tests.

The sintered microstructure of the fractured surfaces was evaluated by scanning electron microscopy via secondary electron images (SEM/SEI) operating at 15 kV (model SEM SSX-550, Shimadzu), after

metallization with a thin layer of gold. FTIR analysis was carried out with a Spectrum 400 FTIR spectrophotometer (model Spectrum 400 FTIR, Perkim-Elmer) in the range from 400 cm^{-1} to 4000 cm^{-1}.

3. Result and discussion

The FTIR spectra of the β-CPP pellets sintered at different temperatures are presented in Figure 3. For comparison, the FTIR spectrum for the green β-CPP pellet (as-synthesized powder pressed at room temperature) was also presented. All FTIR spectra were found to be quite similar, regardless of the sintering temperature. This indicates that thermal degradation of the β-CPP bioceramic during the sintering process did not occur. In fact, the β-CPP powder derived from eggshell waste was found to be stable up to 1100°C with very low weight loss (~ 0.08%) [29]. However, the polymorphic transformation β-CPP (tetragonal structure) → α-CPP (orthorhombic structure) takes place above 900°C [7,25]. Apparently, this polymorphic transformation did not influence the frequency bands of the CPP material during sintering. This is likely connected to the similarity of the frequency bands between the corresponding β-CPP and α-CPP crystalline phases. Thus, the identified frequency bands related to vibrational groups of sintered β-CPP pellets could be interpreted as follow [9,17,30]. It can be seen a broad band centered about at 3404 cm^{-1} to 3490 cm^{-1} and another weak band at 1631 cm^{-1} to 1638 cm^{-1} that corresponds to binding mode of adsorbed H_2O. The bands detected at 962 cm^{-1} to 966 cm^{-1}, 1110 cm^{-1} to 1116 cm^{-1}, 1040 cm^{-1} to 1046 cm^{-1}, and 1121 cm^{-1} to 1125 cm^{-1} are due to the symmetric P-O stretching of PO_3^{-2} groups. The frequency bands detected at 721 cm^{-1} to 725 cm^{-1} and 890 cm^{-1} to 893 cm^{-1} may be related to the asymmetric C-O stretching of CO_3^{-2} group, particularly due to the existence of carbonate in residual level. This result is very similar to that of previous studies [31,32] that detected the CO_3^{-2} band in calcium phosphate bioceramics sintered at high temperature. Finally, the frequency bands detected around 452 cm^{-1} to 456 cm^{-1}, 481 cm^{-1} to 486 cm^{-1}, 580 cm^{-1} to 585 cm^{-1}, and 620 cm^{-1} to 625 cm^{-1} are due to the asymmetric O-P-O stretching of PO_4^{-2} group.

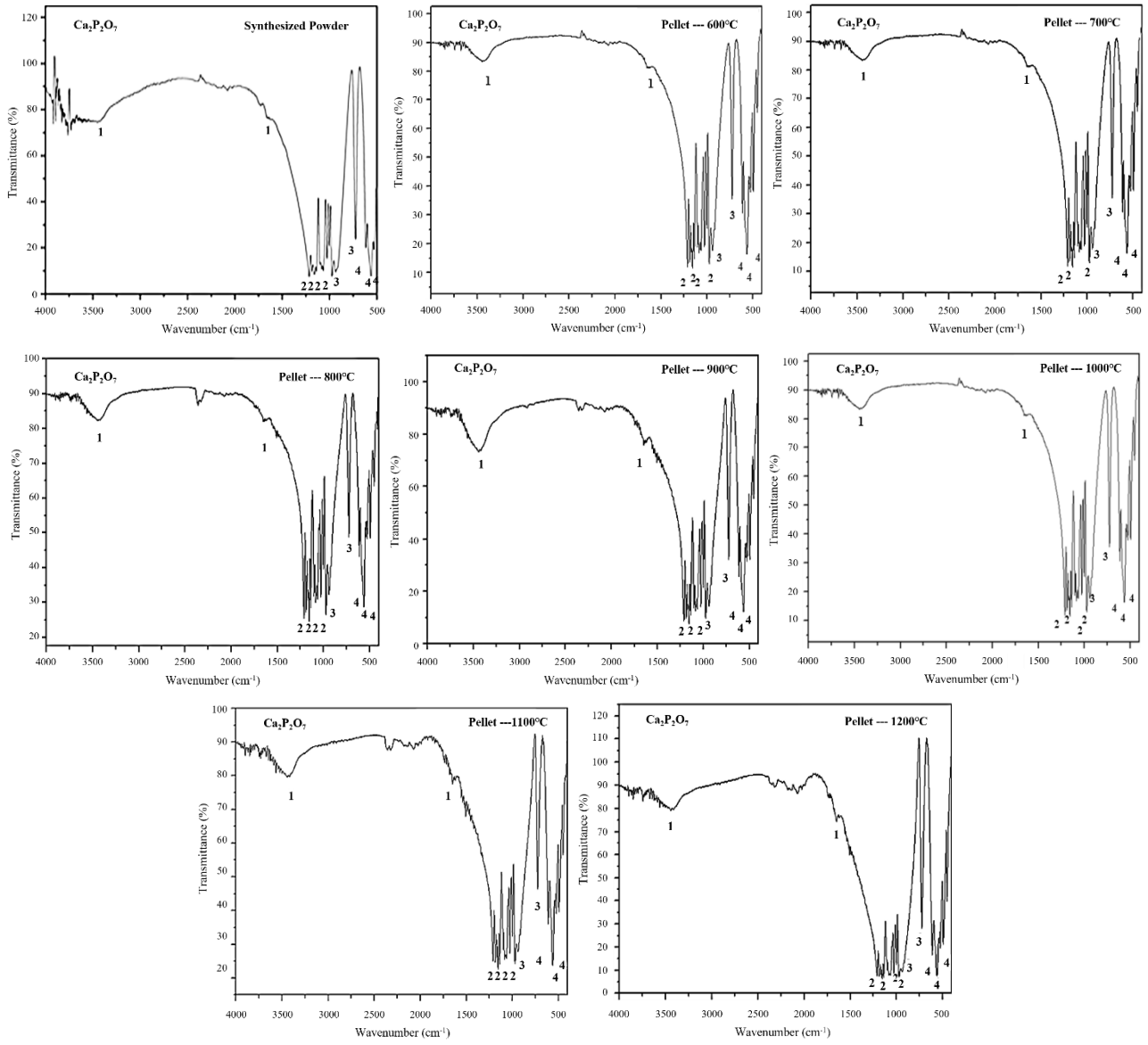

Figure 3. FTIR spectra of the as-synthesized β-CPP powder and sintered pellets at different temperatures: 1 – H_2O; 2 – PO_3^{-2}; 3 – CO_3^{-2}; 4 – PO_4^{-2}.

Figure 4(a-g) shows SEM/SEI images of the fractured surfaces of β-CPP pellets sintered at various temperatures. The effect of the sintering temperature was to cause a significant microstructural variation in the sintered pellets. At 600ºC (Figure 4(a)) and 700°C (Figure 4(b)), the fractured surfaces showed a porous microstructure. In this case, the β-CPP pellets were not well sintered. The observed open porosity is the result of poor solid sintering between the interparticle necks. A further increase in temperature up to 800°C (Figure 4(c)), however, the open porosity started to reduce. At 900°C (Figure 4(d)), a significant amount of open porosity has already been eliminated, resulting in a denser microstructure. Between 1000°C and 1200°C (Figure 4(e-g)), the pellets presented advanced sintering stage and highly densified microstructure. A transgranular fracture surface with strong bonds between the grains can be seen. However, the appearance of micro-cracks in the sintered microstructure was observed. These micro-cracks are mainly associated with the phase transformation β-CPP → α-CPP, since these phases have different densities ($\rho = 3.09\ g{\cdot}cm^{-3}$ for β-CPP and $\rho = 2.95\ g{\cdot}cm^{-3}$ for α-CPP) [33] that under cooling generate differential shrinkage and micro-cracks in the sintered microstructure. Therefore, a negative influence the mechanical strength of sintered β-CPP pellets should be expected.

Figure 5 shows the linear shrinkage of the sintered β-CPP pellets. As may be observed, the β-CPP pellets presented linear shrinkage values ranging from 0.17% to 10.13%. The results also showed that the linear shrinkage presented different behaviors, depending on the sintering temperature. This finding is due to the predomination of different sintering mechanisms. The β-CPP pellets had low linear shrinkage up to 700°C (0.17% to 0.29%), indicating that surface diffusion [18,34] is probably the predominant sintering mechanism. In this temperature range, sintering can essentially be attributed to the formation of interparticle necks accompanied by a high reduction of specific surface area due to the nano sized β-CPP powder used. Above 700°C, however, the sintering of the nano sized β-CPP powder accelerates and a relevant linear shrinkage variation (7.47% to 10.13%) occurs. This behavior is related to grain growth and elimination of a substantial amount of open porosity. In this case, the pellets are prevalently sintered by volume diffusion and/or grain boundary diffusion mechanisms [18]. Such sintering mechanisms are more effective for material densification than for surface diffusion.

Figure 6 shows the variation of the water absorption with the sintering temperature. The water absorption indicates the volume of open pores, that is, the pores that are related with the sintered pellet surface. The measured values of water absorption were in the range of 3.0% to 14.0%. The effect of the sintering temperature was to cause a substantial reduction in the water absorption of the sintered pellets. At lower temperatures (600°C to 700°C) the pellets are characterized by an open pore structure, which then evolve at higher temperatures (above 900°C) to a more compact pellet. This is in accordance with microstructural evolution (Figure 4), linear shrinkage (Figure 5), and apparent porosity (Figure 7).

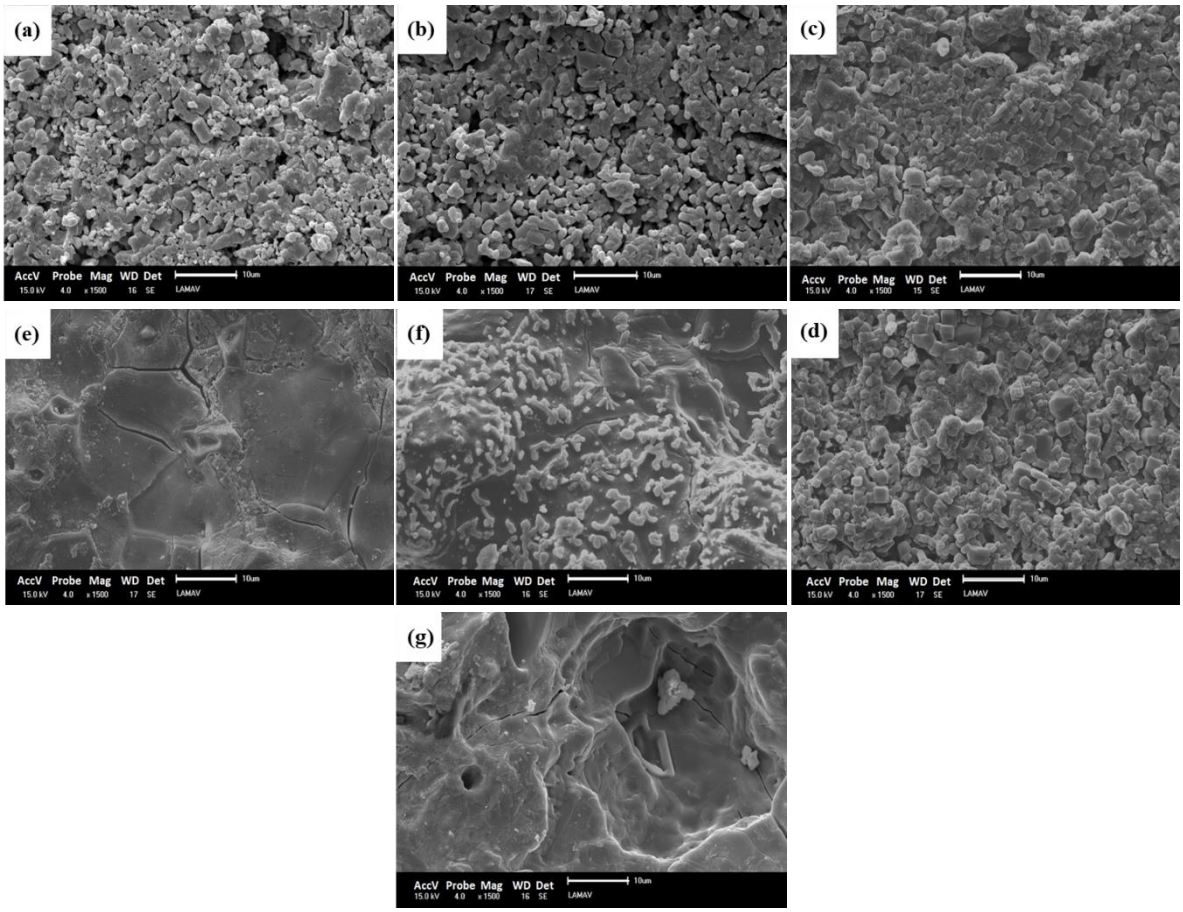

Figure 4. SEM micrographs of the fracture surfaces of the sintered β-CPP pellets: (a) 600°C, (b) 700°C, (c) 800°C, (d) 900°C, (e) 1000°C, (f) 1100°C, and (g) 1200°C.

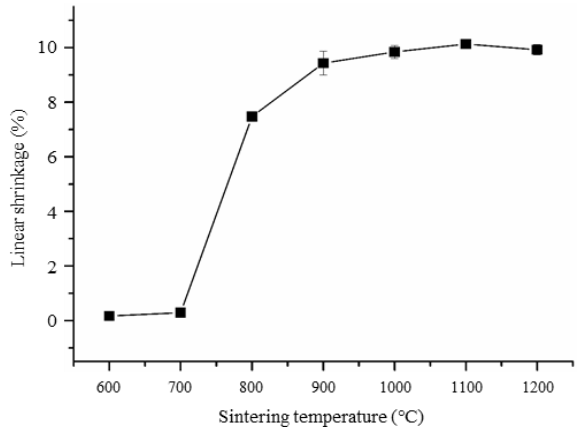

Figure 5. Linear shrinkage of the sintered pellets.

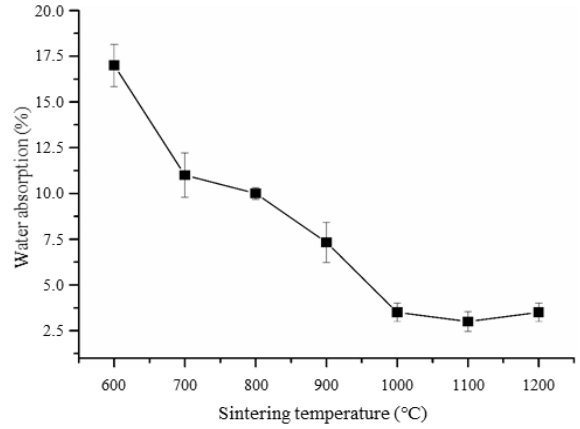

Figure 6. Water absorption of the sintered pellets.

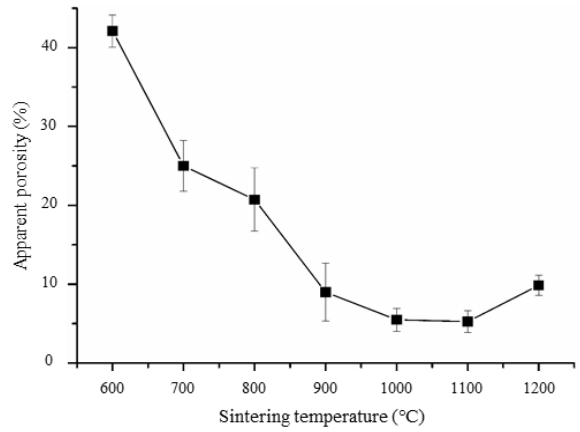

Figure 7. Apparent porosity of the sintered pellets.

The apparent density of the sintered pellets is shown in Figure 8. It was found that the apparent density of the β-CPP pellets increases with increasing sintering temperature up to 1000°C. At this temperature, the maximum apparent density of the sintered pellets of 2.86 g·cm^{-3} was reached. Such an apparent density value corresponds to 92.56% of the theoretical density (TD) of β-CPP (ρ = 3.09 g·cm^{-3}), as shown in Figure 9. Above 1000°C, however, the apparent density decreased to 2.47 g·cm^{-3} (79.94 % TD) when sintered at 1200°C. This finding may be associated with two main aspects: i) abnormal grain growth in the sintered material; and ii) the β-CPP undergoes phase transformation to α-CPP, which is accompanied by volume expansion [9]. Importantly, the densification degree of β-CPP pellets derived of eggshell waste during sintering obtained in this work was higher than those reported by Safronova *et al.* [9] (87% TD at 900°C and 79% TD at 1000°C and 1100°C) and Wang *et al.* [25] (84.14% TD at 900°C). However, the obtained value was lower than that reported by Bian *et al.* [24] (98% TD at 1150°C). Such differences observed in the degree of densification of the sintered pellets can be explained in terms of the different starting β-CPP powders and sintering conditions employed.

The tensile strength of the sintered β-CPP pellets is shown in Figure 10. It was found that the tensile strength is highly correlated with the other physical properties studied. The tensile strength of the pellets increased as the sintering temperature increased to 900°C. This effect is mainly attributed to the progressive closure of open pores and grain growth during sintering, resulting in a higher degree of densification. Above 900°C, however, the tensile strength decreased mainly at 1200°C. This behavior can be explained by the combined effects of abnormal grain growth and β-CPP → α-CPP polymorphic transformation, which tends to induce volume expansion (*i.e.*, crack formation) in the sintered ceramic matrix. This is in agreements with the sintered microstructure (Figure 3). In fact, it is well known that calcium phosphate bioceramics with large grains are more fragile than those with fine-grained microstructure [35]. The above data suggest that conventional sintering above 900°C should be avoided, because it impairs the mechanical strength of the β-CPP bioceramic pellets

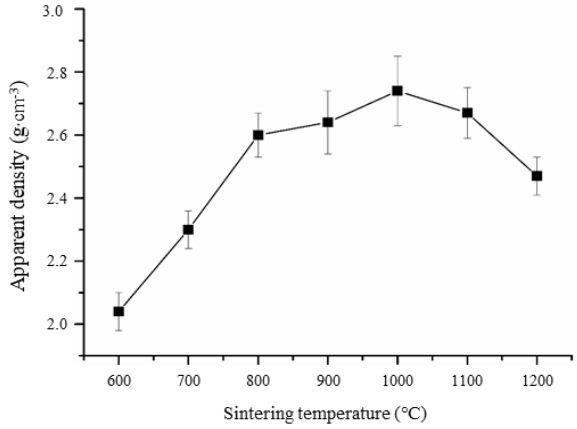

Figure 8. Apparent density of the sintered pellets.

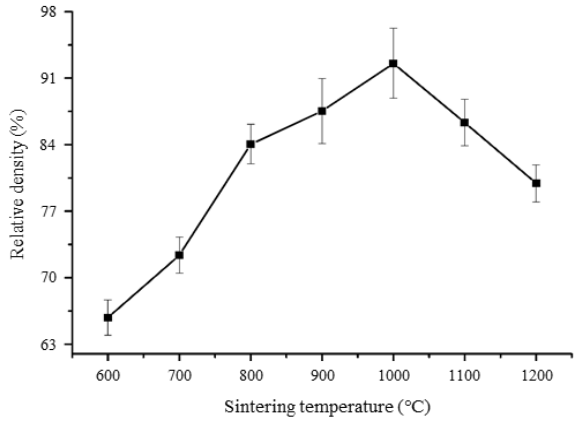

Figure 9. Relative density of the sintered pellets.

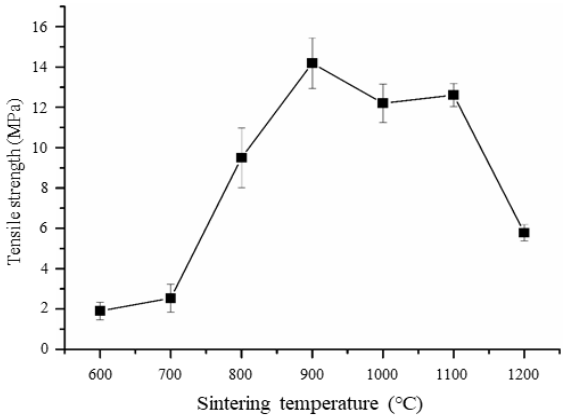

Figure 10. Tensile strength of the sintered pellets.

4. Conclusions

The experimental results of this study indicated that the nano-structured β-CPP powder derived from eggshell waste showed high sinterability characteristics, reaching a high degree of densification. Two sintering regions were found. A good sintering behavior can be achieved above 700°C, which is reflected in higher relative density, higher tensile strength, and denser microstructure. By controlling the sintering temperature at 900°C, β-CPP pellets can be produced with good degree of densification, technical properties, and free of micro-cracks. The results hereby disclosed also suggest that the use of a higher sintering temperature (above 900°C) should not be recommended, as it tends to form a cracked dense microstructure and negatively affects the mechanical strength of the β-CPP bioceramic pellets.

Acknowledgements

The authors acknowledge the Foundation for Research Support of the State of Rio de Janeiro (FAPERJ), Brazil, with the grant number E-26/203.013/2016; and National Council for Scientific and Technological Development (CNPq), Brazil, with the grant number 307507/2019-0 for supporting this work.

References

[1] W. Habraken, P. Habibovic, M. Epple, and M. Bohner, "Calcium phosphates in biomedical applications: materials for the future?," *Materials Today*, vol. 19, no. 2, pp. 69-87, 2016.

[2] S. V. Dorozhkin, "Calcium orthophosphate bioceramics," *Ceramics Inter*national, vol. 41, no. 10, pp. 13913-13966, 2015.

[3] M. E. Gezawi, U. C. Wölfle, R. Haridy, R. Fliefel, and D. Kaisarly, "Remineralization, regeneration, and repair of natural tooth structure: influence on the future of restorative dentistry practical," *ACS Biomaterials Science & Engineering*, vol. 5, no. 10, pp. 4899-4919, 2019.

[4] N. Y. Mostafa, "Characterization, thermal stability and sintering of hydroxyapatite powders prepared by different routes," *Materials Chemistry and Physics*, vol. 94, no. 2-3, pp. 333-341, 2005.

[5] J. S. Sun, Y. H. Tsuang, C. J. Liao, H. C. Liu, Y. S. Hang, and F. H. Lin, "The effects of calcium phosphate particles on the growth of osteoblasts," *Journal of Biomedical Materials Research*, vol. 37, no. 3, pp. 324-334, 1997.

[6] J. H. Lee, D. H. Lee, H. S. Ryu, D. S. Chang, K. S. Hong, and C. K. Lee, "Porous beta-calcium pyrophosphate as a bone graft substitute in a canine bone defect model," *Key Engineering Materials*, vol. 240-242, pp. 399-402, 2003.

[7] S. R. Vasant, and M.,J. Joshi, "Synthesis and characterization of nanoparticles of calcium pyrophosphate," *Modern Physics Letters B*, vol. 25, no. 1, pp. 53-62, 2011.

[8] P. Gras, S. Teychené, C. Rey, C. Chavillat, B. Biscares, S. Sarda, and C. Combes, "Crystallisation of a highly metastable hydrated calcium pyrophosphate phase," *CrystEngComm Journal*, vol. 15, pp. 2294-2300, 2013.

[9] T. V. Safronova, V. I. Putlayev, K. A. Bessonov, and V. K. Ivanov, "Ceramics based on calcium pyrophosphate nanopowders," *Processing and Application of Ceramics*, vol. 7, no. 1, pp. 9-14, 2013.

[10] T. Windarti, A. Haris, Y. Astuti, and A. Darmawan, "Synthesis of β-calcium pyrophosphate by sol-gel method", *IOP Conference Series: Materials Science and Engineering*, vol. 172, pp. 1-7, 2017.

[11] S. R. Vasant, and M. J. Joshi, "A review on calcium pyro-phosphate and other related phosphate nano bio-materials and their applications," *Review on Advanced Materials Science*, vol. 49, no. 1, pp. 44-57, 2017.

[12] P. Pankaew, E. Hoonnivathana, P. Limsuwan, and K. Naemchanthara, "Temperature effect on calcium phosphate synthesized from chicken eggshells and ammonium phosphate," *Journal of Applied Sciences*, vol. 10, no. 24, pp. 3337-3342, 2010.

[13] S. A Osseni, S. A. S. Bonou, E. V. Sogbo, R. Ahouansou, M. Y. Agbahoungbata, D. Neumeyer, M. Verelst, and R. Mauricot, "Synthesis of calcium phosphate bioceramics based on snail shells: towards a valorization of snail shells from Republic of Benin," *American Journal of Chemistry*, vol. 8, no. 4, pp. 90-95, 2018.

[14] S. Owuamanam, and D. Cree, "Progress of bio-calcium carbonate waste eggshell and seashell fillers in polymer composites: A review, *Journal of Composites Science*, vol. 4, no. 2, pp. 1-22, 2020.

[15] A. H. Parsons, "Structure of the eggshell," *Poultry Science*, vol. 61, no. 10, pp. 213-221, 1982.

[16] A. M. Kingóri, "A review of the uses of poultry eggshells and shell membranes," *International Journal of Poultry Science*, vol. 10, no. 11, pp. 908-912, 2011.

[17] T. H. A. Corrêa, and J. N. F. Holanda, "Calcium pyrophosphate powder derived from avian eggshell waste," *Cerâmica*, vol. 62, no. 363, pp. 278-280, 2016.

[18] E. Champion, "Sintering of calcium phosphate bioceramics," *Acta Biomaterialia*, vol. 9, no. 4, pp. 5855-5875, 2013.

[19] B. Mirhadi, "Microwave sintering of nano size powder β-TCP bioceramics," *Science of Sintering*, vol. 46**,** no. 2, pp. 185-193, 2014.

[20] M. Prakasam, J. Locs, K. Salma-Ancane, D. Loca, A. Largeteau, and L. Berzina-Cimdina, "Fabrication, properties and applications of dense hydroxyapatite: a review", *Journal of Functional Biomaterials*, vol. 6, pp. 1099-1140, 2015.

[21] M. A. M. Radzuan, A. B. Sulong, F. M. Foudzi, M. Y. Zakaria, and M. I. Ramli, "Study on the influence mechanism of sintering hydroxyapatite (HA)," *Journal of Ceramic Processing Research*, vol. 21, no. 6, pp. 622-666, 2020.

[22] N. Somers, F. Jean, M. Lasgorceix, H. Curto, G. Urruth, A. Thualt, F. Petit, and A. Leriche, "Influence of dopants on thermal stability and densification of β-tricalcium phosphate powders," *Open Ceramics*, vol. 7, p. 100168, 2021.

[23] A. Indurkar, R. Choudhary, K. Rubenis, and J. Locs, "Advances in sintering techniques for calcium phosphates ceramics," *Materials*, vol. 14, no. 20, pp. 1-18, 2021.

[24] J. J. Bian, D. W. Kim, and K. S. Hong, "Phase transformation and sintering behavior of $Ca_2P_2O_7$," *Materials Letters*, vol. 58, pp. 347-351, 2004.

[25] Q. Wang, Q. Wang, X. Zhang, X. Yu, and C. Wan, "The effect of sintering temperature on the structure and biodegradability of strontium-doped calcium polyphosphate bioceramics," *Ceramics- Silikáty*, vol. 54, no. 2, pp. 97-102, 2010.

[26] J. N. F. Holanda, "Nanostructured calcium phosphate-based bioceramics from waste materials," *in Handbook of Ecomaterials*, ed. Switzerland: Spring International Publishing AG, 2017, pp. 1-18.

[27] T. Fett, "T-stresses in rectangular plates and circular disks," *Engineering Fracture Mechanics*, vol. 60, no. 5-6, pp. 631-652, 1998.

[28] F. Chen, Z. Sum, and J. Shu, "Mode I fracture analysis of the double edge cracked Brazilian disk using a weight function method," *International Journal of Rock Mechanics and Mining Sciences*, vol. 38**,** no. 3, pp. 475-479, 2001.

[29] T. H. A. Corrêa, and J. N. F. Holanda, "Synthesis and characterization of sustainable calcium phosphate nanopowders using eggshell waste," *Trends in Physical Chemistry*, vol. 17, pp. 75-82, 2017.

[30] P. Kamalanathan, S. Ramesh, L. T. Bang, A. Niakan, C. Y. Tan, J. Purbolaksono, and H. Chandran, "Synthesis and sintering of hydroxyapatite derived from eggshell as a calcium precursor," *Ceramics International*, vol. 40, no. 10, pp. 16349-16359, 2014.

[31] D. K. Pattanayak, R. Dash, R. C. Prasad, B. T. Rao, and T. R. Mohan, "Synthesis and sintered properties evaluation of calcium phosphate ceramics," *Materials Science and Engineering: C*, vol. 27, no. 4, pp. 684-690, 2007.

[32] M. Z. A. Khiri, K. A. Matori, M. H. M. Zaid, C. A. C. Abdullah, N. Zainuddin, I. M. Alibe, N. A .A. Rahman, S. A. A. Wahab, A. Z. K. Azman, and N. Effendy, "Crystallization behavior of low-cost biphasic hydroxyapatite/β-tricalcium phosphate ceramic at high sintering temperatures derived from high potential calcium waste sources," Results in Physics, vol. 12, pp. 638-644, 2019.

[33] C. Calvo, "The crystal structure of α-$C_2P_2O_7$," *Inorganic Chemistry*, vol. 7, no. 7, pp. 1345-1351, 1968.

[34] J. E. Blendell, and W. Rheinheimer, "Solid-state sintering," *in Encyclopedia of Materials: Technical Ceramics and Glasses*, ed. Elsevier, 2021, pp. 249-257.

[35] M. Yetmez, "Sintering behavior and mechanical properties of biphasic calcium phosphate bioceramics," *Advances in Materials Science and Engineering*, vol. 2014, pp. 1-5, 2014.